Magnetic and structural characterization of Mn-implanted, single-crystal $ZnGeSiN_2$

S. J. Pearton,[a] M. E. Overberg, and C. R. Abernathy
Department of Materials Science and Engineering, University of Florida, Gainesville, Florida 32611

N. A. Theodoropoulou and A. F. Hebard
Department of Physics, University of Florida, Gainesville, Florida 32611

S. N. G. Chu
Agere Systems, Murray Hill, New Jersey 07974

A. Osinsky, V. Fuflyigin, and L. D. Zhu
Corning Applied Technologies, Woburn, Massachusetts 01801

A. Y. Polyakov
Institute of Rare Metals, Moscow, Russia

R. G. Wilson
Consultant, Stevenson Ranch, California 93181

(Received 29 October 2001; accepted for publication 9 May 2002)

Epitaxial layers of $ZnSiN_2$, $ZnGe_{0.65}Si_{0.35}N_2$, and $ZnGe_{0.31}Si_{0.69}N_2$ grown on Al_2O_3 substrates were implanted at 350 °C with high doses (5×10^{16} cm^{-2}) of Mn^+ ions and annealed at 700 °C. The implanted region did not appear to become amorphous and showed strong selected area diffraction patterns. Hysteresis was observed in magnetization versus field curves from all of the implanted samples. Differences in field-cooled and zero field-cooled magnetization persisted to temperatures of ~200 K for $ZnSiN_2$, and ~280 K for both $ZnGe_{0.31}Si_{0.69}N_2$ and $ZnGe_{0.69}Si_{0.31}N_2$. The results are consistent with recent magnetic data from $(Zn_xMn_{1-x})GeP_2$, $ZnSnAs_2$ and $(Cd_xMn_{1-x})GeP_2$ and suggest that this class of materials may be promising for dilute magnetic semiconductor applications. [DOI: 10.1063/1.1490621]

INTRODUCTION

There is strong current interest in the synthesis of dilute magnetic semiconductors by introducing magnetic ions into a variety of host materials.[1–14] The magnetization of ferromagnetic semiconductors can be manipulated through applied electric fields or changes in carrier density through doping or illumination by photons.[1] These latter phenomena indicate that the ferromagnetism is mediated by charge carriers. A mean field theory by Dietl *et al.*[15] suggested that the ferromagnetism in these materials occurs due to carrier-localized spin exchange between magnetic and carrier polarizations, i.e., there is spin coupling between Mn spins and carrier spins. The double-exchange mechanism discussed in Refs. 4–6 and 16 also has some experimental support, while various aspects of the unusual spin and charge transport have been explained by the presence of positional disorder[17] or spin-glass freezing.[18]

While materials such as (Ga,Mn)As and (In,Mn)As have been the most-studied systems, their Curie temperatures (T_C) are <110 K [with values of 10 K or less for (In,MnAs)].[2,3,19] Room temperature ferromagnetism has been reported in $(Cd_{0.95}Mn_{0.05})GeP_2$,[20] $(Zn_{1-x}Mn_x)GeP_2$,[21,22] GaMnN,[23,24] GaMnP,[25] and $ZnSnAs_2$,[26] consistent with the view that wide band gap semiconductors are the most promising for obtaining high T_C values.[15] The wide band gap II–VI-N_2 semiconductors $ZnGeN_2$ and $ZnSiN_2$ have lattice parameters close to those of GaN and SiC, respectively.[27–31] The achievement of ferromagnetism in these materials would make it possible for direct integration of magnetic sensors and switches with blue/green lasers and light-emitting diodes, UV solar-blind detectors and microwave power electronic devices fabricated in the GaN and SiC. The band gap of $ZnGe_xSi_{1-x}N_2$ varies linearly with the composition from 3.2 ($x=1$) to 4.46 eV ($x=0$),[27–33] and breakdown fields above 10^6 V cm^{-1} have been reported.[28] Moreover, these materials possess promising nonlinear optical coefficients.[27–31] In this article we report on the magnetic and structural properties of Mn-implanted $ZnSiN_2$ and $ZnGeSiN_2$ single-crystalline films grown on *r* sapphire. These materials also appear to have great promise for achieving practical ferromagnetic ordering temperatures.

EXPERIMENT

The films were grown on low temperature GaN buffers on *r*-plane sapphire substrates by metalorganic chemical vapor deposition using conditions reported previously.[27–29,31] In brief, germane and silane were used as the group IV sources, ammonia as the nitrogen source and tetraethyl zinc as the group II source. The growth temperature was in the range of 650–800 °C. The epi thickness was ~0.8 μm, with orthorhombic symmetry. The films were nominally undoped,

[a]Electronic mail: spear@mse.ufl.edu

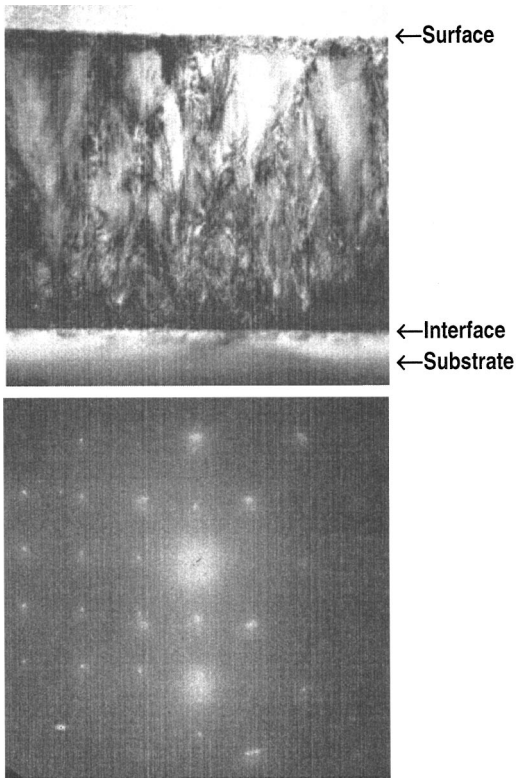

FIG. 1. TEM cross section (top) and SADP (bottom) of $ZnSiN_2$ grown on sapphire and implanted with Mn^+ at a dose of 5×10^{16} cm^{-2} and then annealed at 700 °C. The epi layer thickness is 0.8 μm, which sets the scale.

with a low *n*-type background that appears to come from unintentional incorporation of donor impurities that are present in the precursors.

Mn^+ ions were implanted at a dose of 5×10^{16} cm^{-2} and energy 250 keV, with the substrates held at ~350 °C to avoid amorphization.[34,35] From secondary ion mass spectrometry (SIMS) measurements, the projected range of these ions is roughly 1500 Å and follows a Gaussian profile that is slightly skewed towards the surface due to associated sputtering that occurs at such high doses. The peak Mn concentration was measured to be approximately 5 at. % from these SIMS measurements, using lower dose implants (10^{15} cm^{-2}) as a calibration standard. Following implantation, the samples were annealed at 700 °C for 5 min under flowing N_2, with the $ZnGeSiN_2$ face down on GaN samples. The structural properties of the implanted material were examined by cross-sectional transmission electron microscopy (TEM) and selected area diffraction patterns (SADPs), while the magnetic properties were measured with a Quantum Design superconducting quantum interference device (SQUID) magnetometer.

RESULTS AND DISCUSSION

Figure 1 (top) shows a cross-sectional TEM micrograph of the $ZnSiN_2$ after Mn^+ implantation and annealing. There is a high density of threading dislocations that originate in the lattice mismatch between the nitride and the sapphire substrate but no defective region due to incomplete regrowth of a heavily damaged surface layer, such as what would be present if the Mn implant had partially or completely amorphized the $ZnSiN_2$.[34–37] It is very unlikely, given the complexity of the chalcopyrite lattice structure and the fact it contains four different elements, that solid-phase regrowth of such a damaged region would be successful. The SADP of the entire structure (epi plus substrate) showed just the lattice spots that were present prior to the implant (Fig. 1, bottom) indicating that no secondary phase formation occurred, at least to the sensitivity of electron diffraction. The SADP pattern does show evidence of streaking due to the presence of residual lattice disorder, but no additional spots. A careful examination of the implanted region by TEM also showed there were no precipitates or secondary phases present to within the resolution of the instrument (25 Å). The blocking temperature of superparamagnetic particles of this size would be expected to be <10 K based on a simple calculation.[12] Additional ferromagnetic phases that might be expected to form in heavily Mn-implanted material include Mn_3N_2 with a tetragonal lattice structure and Mn_4N with a cubic structure. However, these were not observed and the magnetic behavior discussed below was not consistent with their being present. We still cannot categorically rule out the presence of very small (a few atom spacings) magnetic clusters of the type proposed recently to account for ferromagnetism in some semiconductor systems.[38] The Mn in solution can substitute for Zn, Ge or Si, but analogous to previous reports, we assume it resides mainly on Zn lattices positions.[21,26]

Figure 2 shows magnetization versus field curves measured at 10 (top) and 100 K (bottom). There is hysteresis evident at both temperatures, although the curves do not show saturation at the maximum field investigated (1000 G). Although ferromagnetism is the usual explanation for hysteresis, other causes could be superparamagnetism or spin-glass effects.[2,3,12] In other semiconductor systems implanted with Mn we observe saturation of the magnetization at fields above 2 k Oe.[36,37] The Mn implantation into $ZnSiN_2$ clearly causes a major change in the magnetic properties, because the unimplanted material was diamagnetic. To confirm the presence of magnetization in the samples, field-cooled and zero field-cooled measurements were performed using an applied field in the former case that was less than the anisotropy fields associated with the samples at the lowest temperatures. These experiments confirmed a divergence in the two traces for temperatures below approximately 200 K.

Figure 3 shows this difference in magnetization between field-cooled (FC) and zero field-cooled (ZFC) conditions as a function of the temperature. The ferromagnetic contribution is present up to ~200 K in these Mn-implanted $ZnSiN_2$ samples. As discussed above, there do not appear to be second phases in the material which would produce additional contributions to the magnetization. The shape of the curve is consistent with the predictions in Ref. 17 for materials containing disordered regions. The difference in field-cooled and zero field-cooled traces could have its origin in a number of different mechanisms. For example, the presence of superparamagnetic clusters in the implanted region would produce this effect. However, the size of these clusters would have to be at least on the order of a few tens of nanometers to pro-

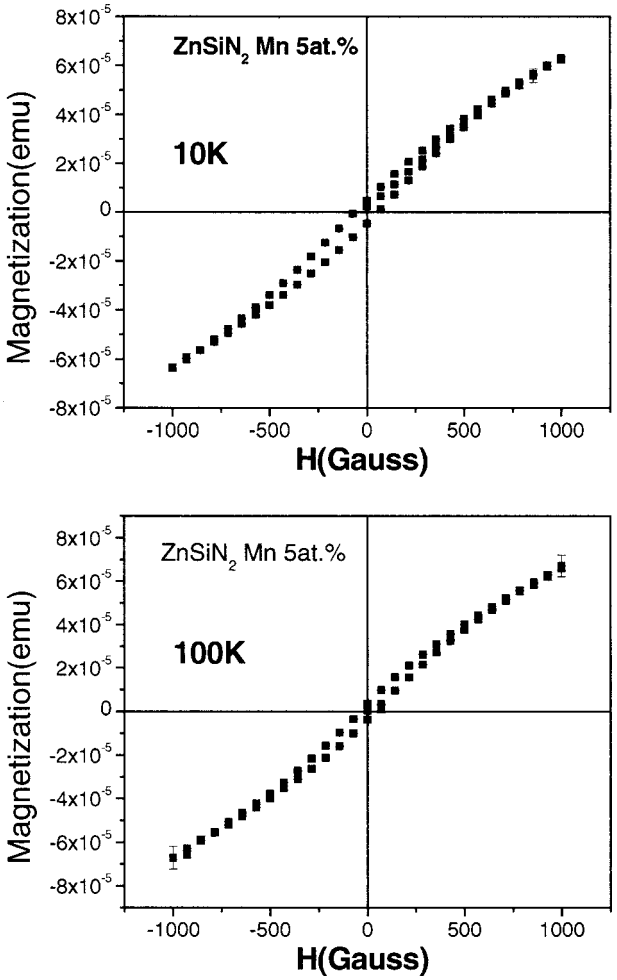

FIG. 2. Magnetization curves at 10 (top) or 100 K (bottom) of $ZnSiN_2$ implanted with Mn^+ and annealed at 700 °C.

duce a blocking temperature around 200 K,[39] and no clusters of this size were visible in the high resolution TEM images. Second, if the materials behave as spin glass, there would be differences in the field-cooled and zero field-cooled traces.

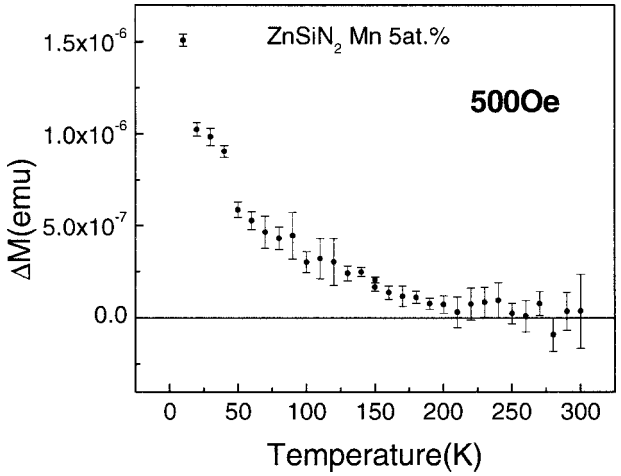

FIG. 3. Temperature dependence of the difference between field-cooled and zero field-cooled magnetization for $ZnSiN_2$ implanted with 5×10^{16} cm^{-2} Mn^+ and annealed at 700 °C.

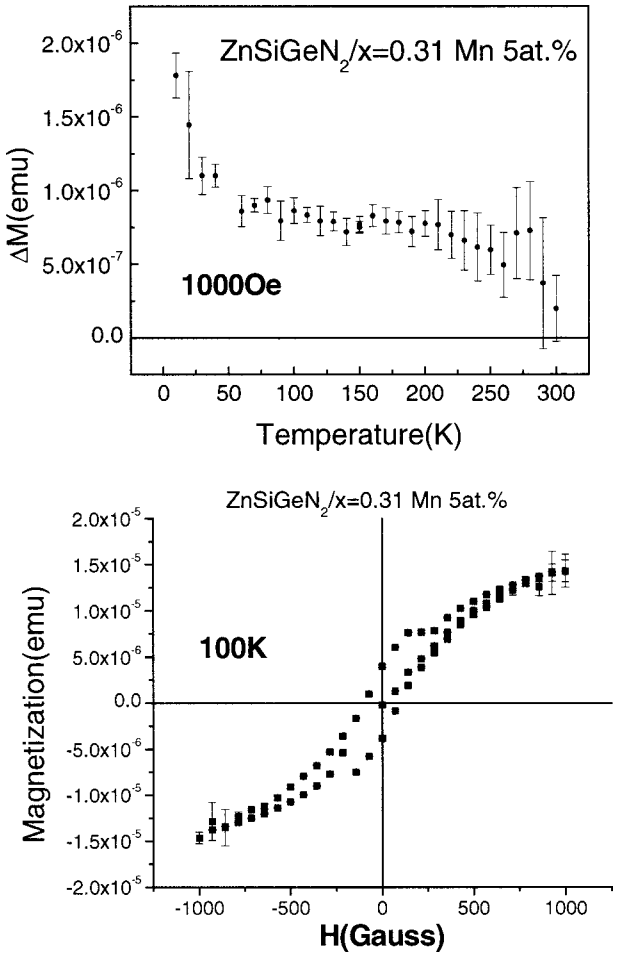

FIG. 4. Temperature dependence of the difference between field-cooled and zero field-cooled magnetization for $ZnGe_{0.31}Si_{0.69}N_2$ implanted with 5×10^{16} cm^{-2} Mn^+ and annealed at 700 °C (top) and magnetization curve at 100 K of the same sample (bottom).

However, the samples show clear remanent magnetization and no cusp is apparent in the M vs T measurements. In future work we will try to establish the dependence of the ordering temperature on the Mn concentration and the conductivity type and level of $ZnSiN_2$. The T_C of the $Zn_{1-x}Mn_xGeP_2$ reported previously was 312 K for material that was insulating.[21]

In $ZnSiGeN_2$ ternary alloys we observed slightly higher ordering temperatures than for $ZnSiN_2$, even though their band gap is slightly smaller. Figure 4 (top) shows the temperature dependence of the difference between FC and ZFC magnetization for $ZnGe_{0.31}Si_{0.69}N_2$ samples implanted with Mn and annealed at 700 °C. The apparent ordering temperature is ~280 K. The magnetization curve at 100 K is shown at the bottom of Fig. 4. The diamagnetic background was subtracted from the magnetization curve. Once again, these data could be interpreted either by the presence of two different contributions to the magnetization or by the presence of disordered regions.[17]

Similar data are shown in Fig. 5 for the Mn-implanted $ZnGe_{0.65}Si_{0.35}N_2$ layers. The apparent ordering temperature is again ~280 K (Fig. 5, top), while the coercive field at 10 K is 185 ± 35 G. The band gap of this material is 3.52 eV

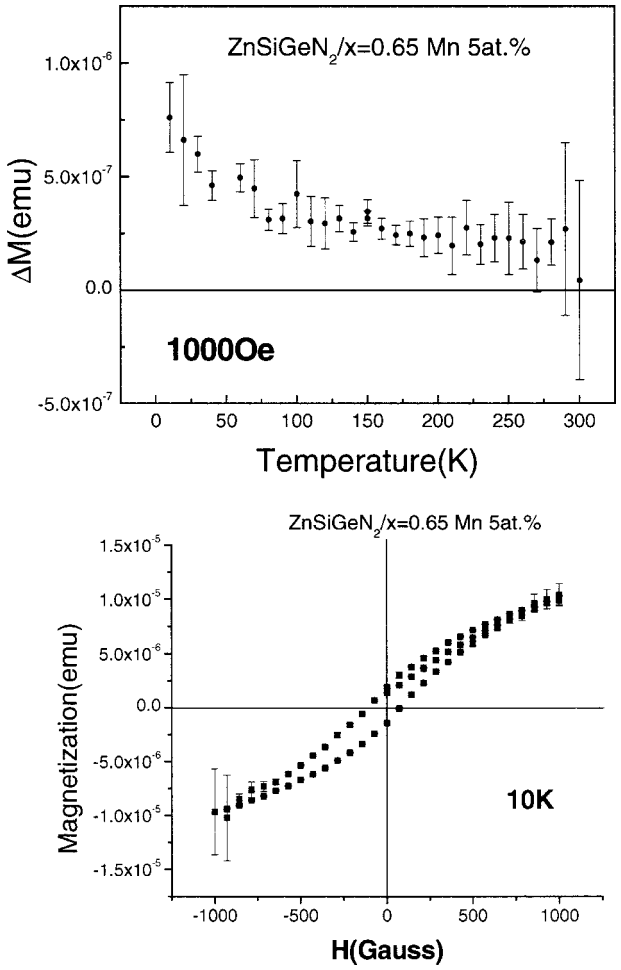

FIG. 5. Temperature dependence of the difference between field-cooled and zero field-cooled magnetization for $ZnGe_{0.65}Si_{0.35}N_2$ implanted with 5 $\times 10^{16}$ cm^{-2} Mn^+ and annealed at 700 °C (top) and magnetization curve at 10 K of the same sample (bottom).

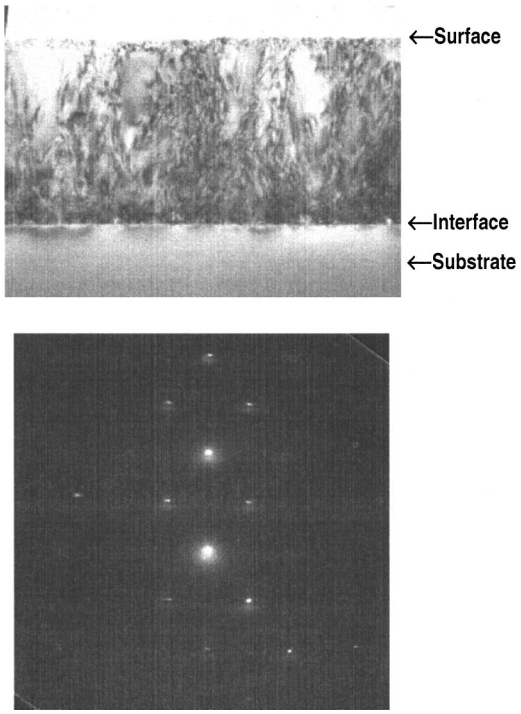

FIG. 6. TEM cross section (top) and SADP (bottom) of $ZnGe_{0.65}Si_{0.35}N_2$ implanted with Mn^+ at a dose of 5×10^{16} cm^{-2} and annealed at 700 °C. The epi layer thickness is 0.8 μm, which sets the scale.

compared to 3.93 eV for the $ZnGe_{0.31}Si_{0.69}N_2$ composition, but there is no significant difference in apparent ordering temperature between the two samples.

A TEM cross-sectional micrograph and a SADP from the Mn-implanted $ZnGe_{0.65}Si_{0.35}N_2$ are shown in Fig. 6. In this case the SADP is from the epi layer only. Other potential phases that could form are Mn_3N_2 (which has tetragonal symmetry, $a=2.966$ Å and $c=12.243$ Å) and Mn_4N (which has cubic symmetry, $a=3.846$ Å), but both of these would give rise to extra spots in the diffraction pattern and clearly they are not present according to the sensitivity of our characterization techniques. Once again, no precipitates or clusters were visible to within a resolution of approximately 25 Å.

SUMMARY AND CONCLUSIONS

The development of wide band gap II–IV-N_2 semiconductors compatible with group III nitrides may produce integrated devices with multiple functionalities. We have found that $ZnSiN_2$ and $ZnGeSiN_2$ implanted with Mn at doses designed to produce a peak Mn concentration of ~5 at. % show magnetic ordering temperatures in the range of 200–280 K. The mechanism for the magnetic behavior is not clear, since carrier-induced ferromagnetism is expected to require very high carrier concentrations and our samples are lightly *n* type at room temperature. Ion implantation appears to be an effective method by which to introduce the Mn, and the $ZnGeSiN_2$ is not amorphized by the heavy dose employed here. This material system looks quite promising for magnetic applications.

ACKNOWLEDGMENTS

The work at the University of Florida was partially supported by NSF Grant Nos. DMR-0101438 and DMR-9705224 and by the U.S. Army under Contract No. ARO DAAD19-01-1-0701. The work of one of the authors (R.G.W.) was also partially supported by ARO.

[1] T. Dietl, J. Appl. Phys. **89**, 7437 (2001); T. Dietl, H. Ohno, and F. Matsukura, Phys. Rev. B **63**, 195205 (2001).
[2] H. Ohno, J. Magn. Magn. Mater. **200**, 110 (1999); Science **281**, 951 (1998).
[3] T. Story, Acta Phys. Pol. A **91**, 173 (1997).
[4] S. Katsumoto *et al.*, Mater. Sci. Eng., B **84**, 88 (2001).
[5] H. Akai, Phys. Rev. Lett. **81**, 3002 (1998).
[6] J. Okabayashi, A. Kimura, T. Mizokawa, A. Fujimori, T. Hayashi, and M. Tanaka, Phys. Rev. B **58**, R4211 (1998).
[7] G. A. Prinz, Science **282**, 1660 (1998).
[8] B. T. Jonker, Y. D. Park, B. R. Bennet, H. D. Cheong, G. Kioseoglou, and A. Petrou, Phys. Rev. B **62**, 8180 (2000).
[9] Y. D. Park, B. T. Jonker, B. R. Bennet, G. Itkos, M. Furis, G. Kioseoglou, and A. Petrou, Appl. Phys. Lett. **77**, 3989 (2000).
[10] W. Gebicki, J. Strzeszewski, G. Kamler, T. Szysko, and S. Podliasko, Appl. Phys. Lett. **76**, 3870 (2000).
[11] M. Zajac *et al.*, Appl. Phys. Lett. **78**, 1276 (2001).
[12] F. Holzberg, S. von Molnar, and J. M. D. Coey, in *Handbook on Semiconductors*, edited by T. S. Moss (North-Holland, Amsterdam, 1980), Vol. 3.

[13] See, for example, the Proceedings of the WTEC Panel on Spin Electronics (www.wtec.org).
[14] Y. D. Park *et al.*, Science **295**, 647 (2002).
[15] T. Dietl, H. Ohno, F. Matsukura, J. Cibert, and D. Ferrand, Science **287**, 1019 (2000).
[16] D. M. Edwards, Mater. Sci. Eng., B **84**, 138 (2001).
[17] M. Berciu and R. N. Bhatt, Phys. Rev. Lett. **87**, 107203 (2001).
[18] J. Jaroszynski and T. Dietl, Mater. Sci. Eng., B **84**, 81 (2001).
[19] H. Ohno, H. Munekata, T. Penney, S. von Molnar, and L. L. Chang, Phys. Rev. Lett. **68**, 2664 (1992).
[20] G. Medvedkin, I. Ishibashi, T. Nishi, K. Hayata, Y. Hasegawa, and K. Sato, Jpn. J. Appl. Phys., Part 2 **39**, L949 (2000).
[21] G. A. Medvedkin, K. Hirose, T. Ishibashi, T. Nishi, V. G. Voevodin, and K. Sato, J. Cryst. Growth **236**, 609 (2002).
[22] S. Cho *et al.*, Phys. Rev. Lett. **88**, 257203 (2002).
[23] M. L. Reed, N. A. El-Masry, H. N. Stadelmaier, M. K. Ritums, M. J. Reed, C. A. Parker, J. C. Roberts, and S. M. Bedair, Appl. Phys. Lett. **79**, 3473 (2001).
[24] G. T. Thaler *et al.*, Appl. Phys. Lett. **80**, 3964 (2002).
[25] N. Theodoropoulou, A. F. Hebard, M. E. Overberg, C. R. Abernathy, S. J. Pearton, S. N. G. Chu, and R. G. Wilson, cond-mat/0201492 (2002).
[26] S. Choi, G. B. Cha, S. C. Hong, S. Cho, Y. Kim, J. B. Ketterson, S. Y. Jeong, and G. C. Yi, Solid State Commun. **122**, 165 (2002).
[27] L. D. Zhu, P. H. Maruska, P. E. Norris, P. W. Yip, and L. O. Bouthillette, Mater. Res. Soc. Symp. Proc. **537**, G3.8 (1999).
[28] S. Limpijumnong, S. N. Rashkeev, and W. L. R. Lambrecht, Mater. Res. Soc. Symp. Proc. **537**, G6.11 (1999).
[29] A. Mintairov, J. Merz, A. Osinsky, V. Fuflyigin, and L. D. Zhu, Appl. Phys. Lett. **76**, 2517 (2000).
[30] R. Viennois, T. Taliercio, V. Potin, A. Ervebbahi, B. Gil, S. Chavar, A. Haidoux, and J.-C. Tedenac, Mater. Sci. Eng., B **82**, 45 (2001).
[31] A. Osinsky, V. Fuflyigin, L. D. Zhu, A. B. Goulakov, J. W. Graff, and E. F. Schubert, Proceedings of the 2000 IEEE/Cornell Conference on High Performance Devices, 2000, p. 168.
[32] W. L. Larson, H. P. Maruska, and D. A. Stevenson, J. Electrochem. Soc. **121**, 1673 (1974).
[33] S. Kikkawa and H. Morisaka, Solid State Commun. **112**, 513 (1999).
[34] J. S. Williams, Mater. Sci. Eng., A **253**, 9 (1998).
[35] S. O. Kucheyev, M. Toth, M. R. Phillips, J. S. Williams, C. Jagadish, and G. Li, Appl. Phys. Lett. **78**, 34 (2001).
[36] N. Theodoropoulou, A. F. Hebard, S. N. G. Chu, M. E. Overberg, C. R. Abernathy, S. J. Pearton, R. G. Wilson, and J. M. Zavada, Electrochem. Solid-State Lett. **4**, G119 (2001).
[37] N. Theodoropoulou, A. F. Hebard, S. N. G. Chu, M. E. Overberg, C. R. Abernathy, S. J. Pearton, R. G. Wilson, and J. M. Zavada, Appl. Phys. Lett. **79**, 3452 (2001).
[38] M. van Schilfgaarde and O. N. Mryasov, Phys. Rev. B **63**, 233205 (2001).
[39] A. Van Esch, Phys. Rev. B **56**, 13103 (1997).